

Deuteron scattering and transfer reactions within NCSM-RGM and NCSMC

Francesco Raimondi, TRIUMF

In collaboration with:
G. Hupin, P. Navrátil, S. Quaglioni

TRIUMF Workshop
19 February 2015
Vancouver, Canada

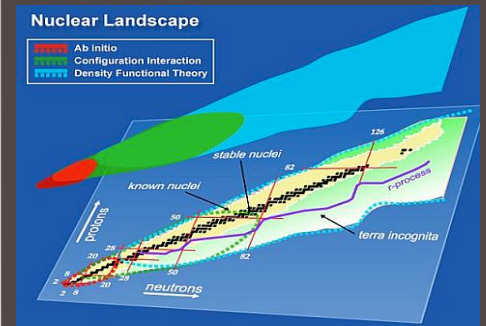
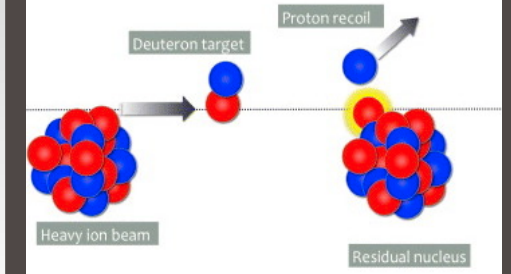


Figure 1 from Kate L Jones 2013 Phys. Scr. 2013 014020

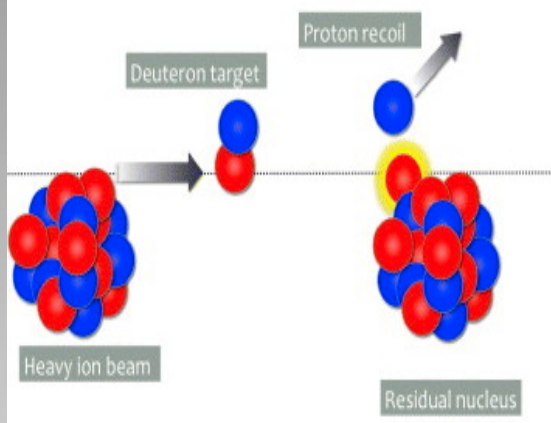


Outline

- ✓ Motivations for *ab initio* study of transfer reactions
- ✓ Interest of ${}^7\text{Li}(d,p){}^8\text{Li}$ reaction
- ✓ Results on the first resonance of ${}^9\text{Be}$ above d - ${}^7\text{Li}$ threshold
- ✓ Recent progress on inclusion of 3N forces in transfer reaction (s-shell nuclei)
(on behalf of: G. Hupin, P. Navrátil, S. Quaglioni)
- ✓ Conclusions

Deuteron-nucleus reaction: experimental motivations

Figure 1 from Kate L Jones 2013 Phys. Scr. 2013 014020



(d,p) reaction in
inverse kinematics

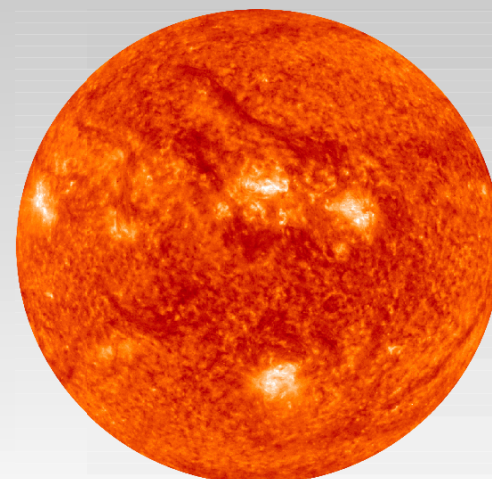
Intense experimental activity (now with exotic nuclei beams in RIB facilities):

- Structure and spectroscopy of nuclei ($^{11}\text{Be}(d,p)^{12}\text{Be}$ at ISAC - TRIUMF)
- Nucleosynthesis and nuclear fusion applications ($^3\text{H}(d,n)^4\text{He}$ reaction)
- Surrogate for (p/n) capture reactions ($^{14}\text{C}(d,p)^{15}\text{C}$ as surrogate of $^{14}\text{C}(\text{n}, \gamma)^{15}\text{C}$)

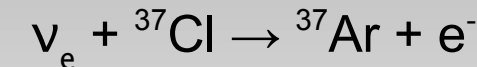
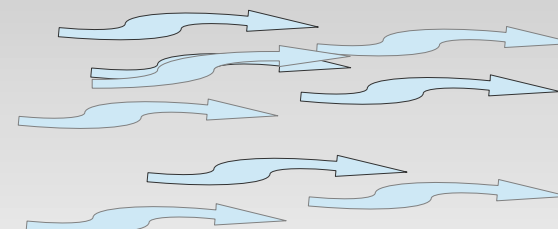
$^7\text{Li}(d,\text{p})^8\text{Li}$ transfer reaction



Calibration reaction for astrophysical process: $^7\text{Li}(d,\text{p})^8\text{Li}$ as target calibration for $^7\text{Be}(\text{p},\gamma)^8\text{B}$



Solar neutrino problem:



R. Davis Jr takes a dip
At Homestake Mine (1971)

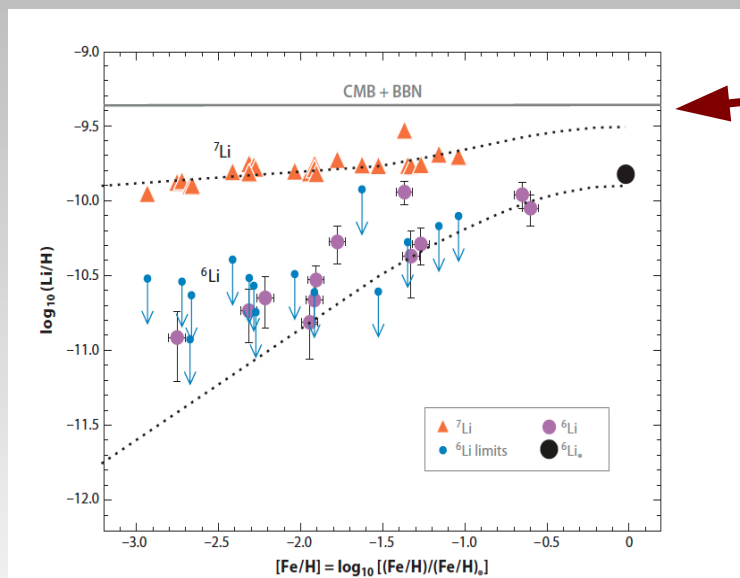
$^7\text{Li}(d,\text{p})^8\text{Li}$ transfer reaction



Calibration reaction for astrophysical process: $^7\text{Li}(d,\text{p})^8\text{Li}$ as target calibration for $^7\text{Be}(\text{p},\gamma)^8\text{B}$

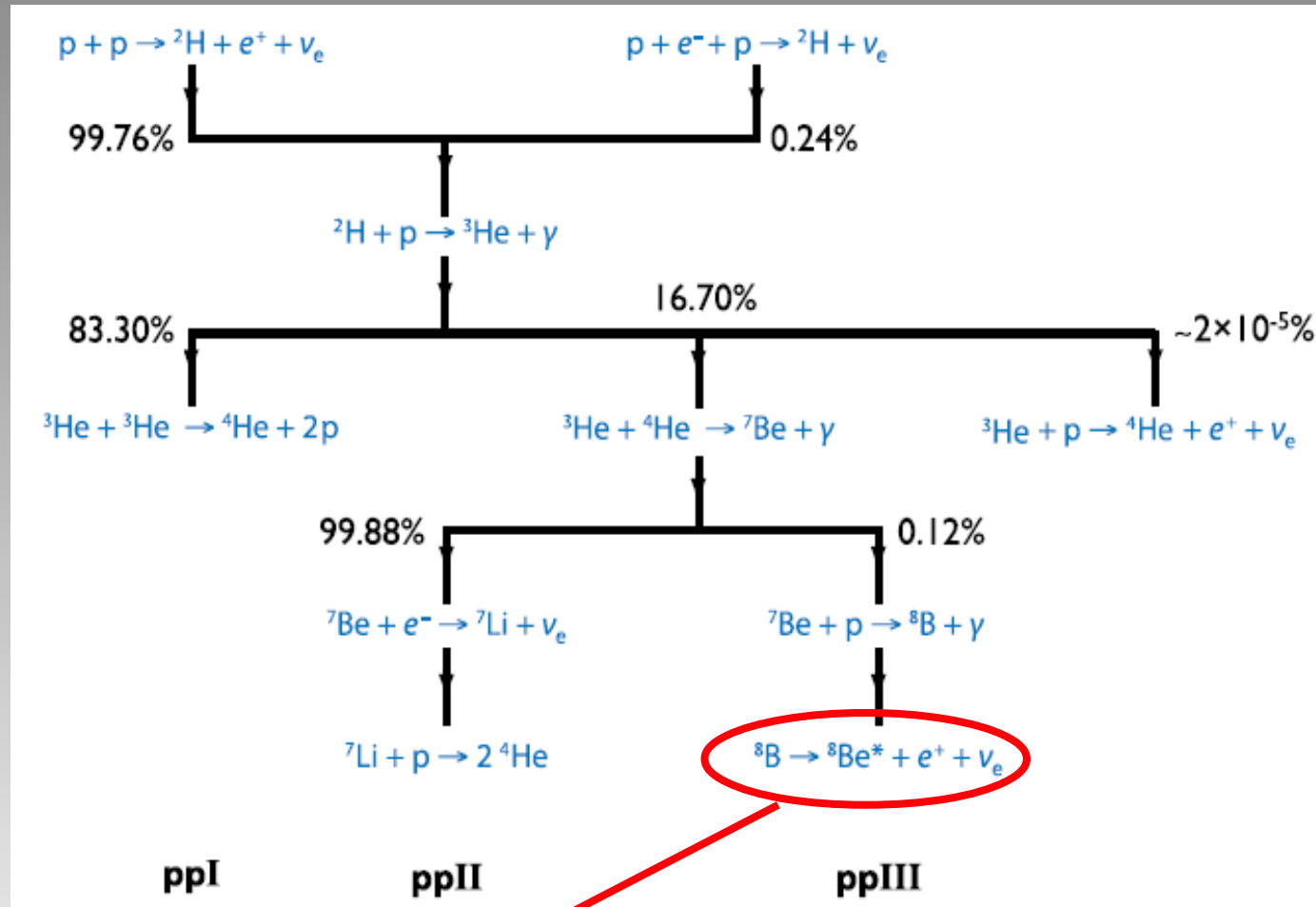


Possible mechanism of destruction of ^7Li in the context of baryon-inhomogeneous models of the primordial nucleosynthesis



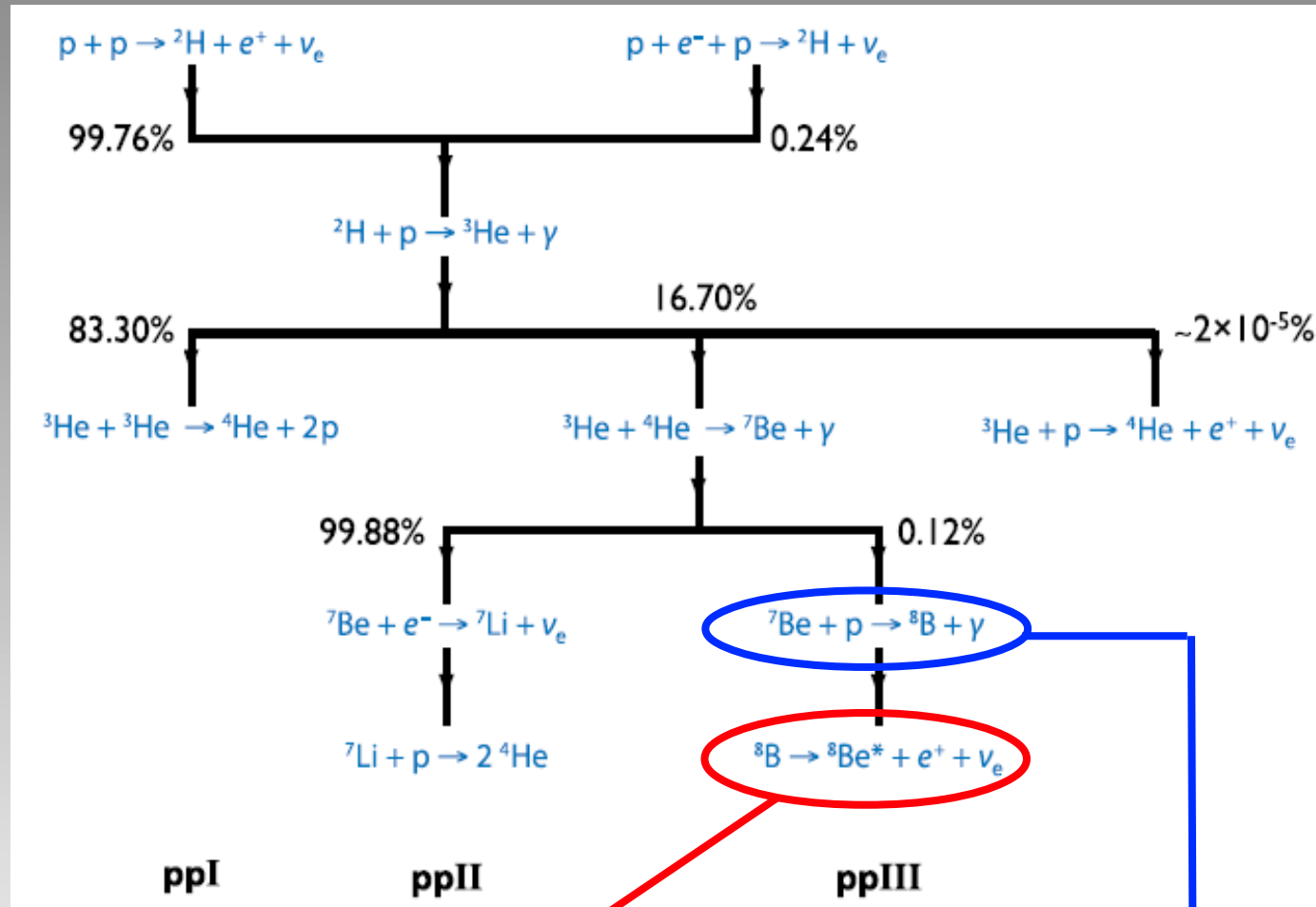
- Primordial Lithium problem:
- $4-5\sigma$ discrepancy between observed and calculated (CMB+BBN) abundance of ^7Li
 - Nuclear solution to the problem: d - ^7Li destruction mechanism is ruled out (but only in a standard BBN scenario PRC 47, 2369 1993)

Solar p-p chain



High-energy solar neutrinos
(E_ν up to 15 MeV)

Solar p-p chain



$S_{17}(0)$ crucial input to estimate solar neutrino flux

High-energy solar neutrinos “Prudent conservative range” $S_{17}(0)=20.8(2.1)$ eV b
 $(E_\nu$ up to 15 MeV) $(\text{Rev Mod Phys } 83, 1 (2011))$

$^{7}\text{Be}(\text{p},\gamma)^{8}\text{B}$ direct measurements

Solar fusion cross sections (Rev Mod Phys 70, 4, 1265 (1998))

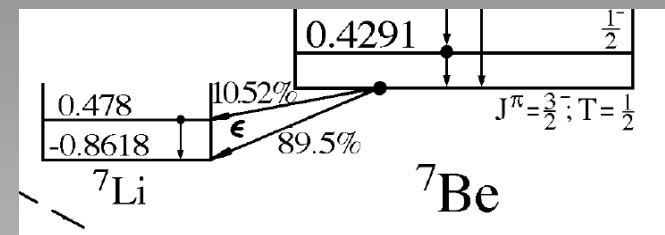
- At low energy, it is an external, direct-capture process ($Q=137.5 \pm 1.2 \text{ KeV}$)
- Experimental uncertainties:
 - Need to be extrapolated to astrophysical relevant regime ($E_p < 134 \text{ KeV}$)
 - ^{7}Be target is radioactive: Areal density of ^{7}Be difficult to estimate (required for normalization of the cross section)
- Two possible strategies:
 - Direct: counting 429 KeV photons of ^{7}Be decay (Filippone 1983)
 - Indirect: measuring the $^{7}\text{Li}(d,p)^{8}\text{Li}$ yield on the resonance ($\Gamma \approx 0.2 \text{ MeV}$) at $E_d = 0.78 \text{ MeV}$) (Kavanagh 1960, Parker 1966, Filippone 1982, Weissman 1998)

${}^7\text{Li}(d,p){}^8\text{Li}$ calibration reaction (Normalization procedure)

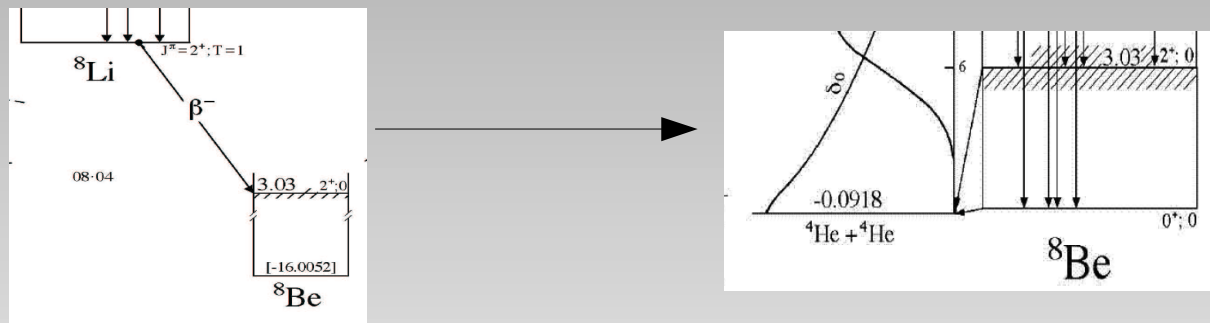
1) Buildup of ${}^7\text{Li}$ in ${}^7\text{Be}$

$$N_{{}^7\text{Li}}(t) = N_{{}^7\text{Be}}(0)(1 - e^{\lambda t}) + N_{{}^7\text{Li}}(0)$$

N_i areal density at time t



2) Counting ${}^7\text{Li}$ through the yield of (d,p) reaction



Beta-delayed
alphas detected

3) Areal density of Li from total σ

$$\sigma(E_d) \sim \frac{Y_\alpha(E)\beta({}^8\text{Li})}{N_d N_{{}^7\text{Li}}(t)}$$

$Y_\alpha(E)$ alpha-particle yield

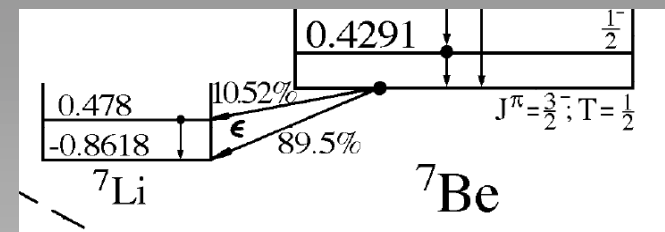
$\beta({}^8\text{Li})$ depends on decay constant of ${}^8\text{Li}$

${}^7\text{Li}(d,p){}^8\text{Li}$ calibration reaction (Normalization procedure)

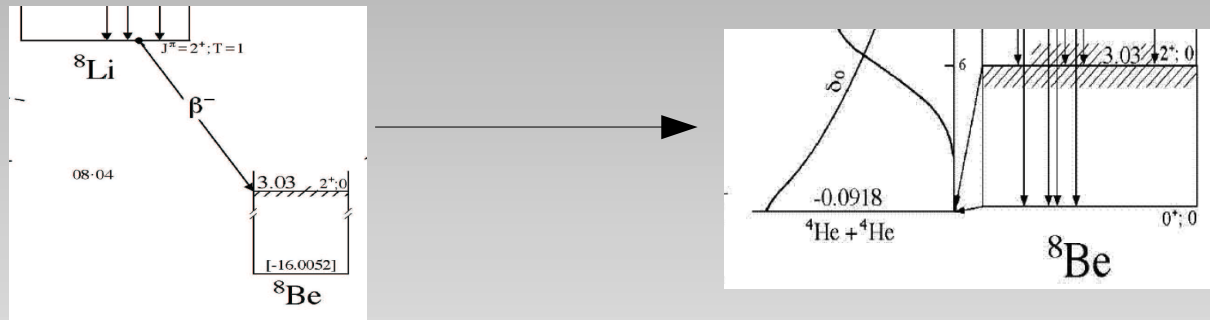
1) Buildup of ${}^7\text{Li}$ in ${}^7\text{Be}$

$$N_{{}^7\text{Li}}(t) = N_{{}^7\text{Be}}(0)(1 - e^{\lambda t}) + N_{{}^7\text{Li}}(0)$$

N_i areal density at time t



2) Counting ${}^7\text{Li}$ through the yield of (d,p) reaction



Beta-delayed
alphas detected

3) Areal density of Li from total σ

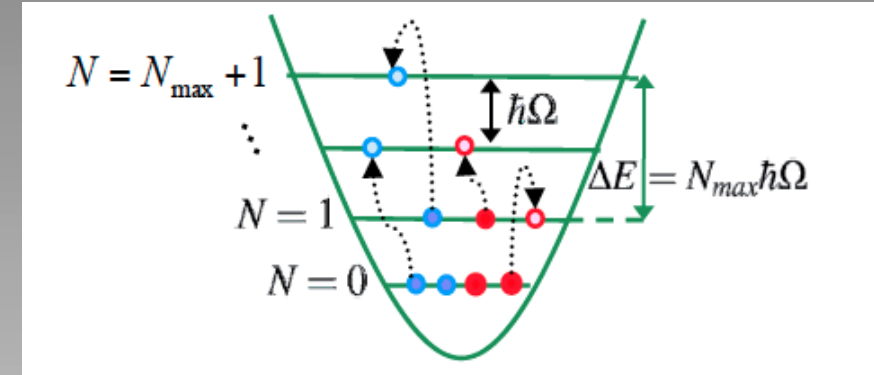
$$\sigma(E_d) \sim \frac{Y_\alpha(E)\beta({}^8\text{Li})}{N_d N_{{}^7\text{Li}}(t)}$$

$Y_\alpha(E)$ α -particle yield

$\beta({}^8\text{Li})$ depends on decay constant of ${}^8\text{Li}$

No-core shell model with continuum

- No-core shell model (NCSM):
 - A-nucleon wave function expansion in the harmonic-oscillator (HO) basis
 - Short- and medium-range correlations
 - Bound states and narrow resonances



$$\Psi^{(A)} = \sum_{\lambda} c_{\lambda} \left| (A) \begin{array}{c} \text{red sphere} \\ \text{blue sphere} \end{array}, \lambda \right\rangle$$

Unknowns

No-core shell model with continuum

- NCSM with Resonating Group Method (NCSM/RGM):

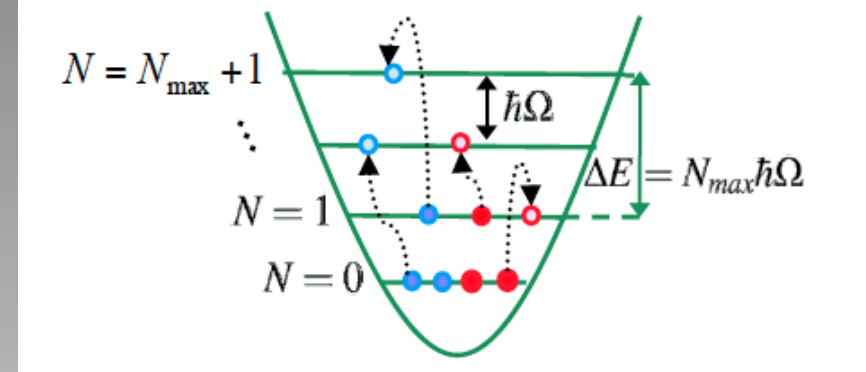
- Cluster expansion
- Proper asymptotic behaviour
- Long-range correlations

$$\Psi^{(A)} = \sum_v \int d\vec{r} \gamma_v(\vec{r}) \hat{A}_v \left|_{(A-a)}^{\vec{r}} (a), v \right\rangle$$

Unknowns 

No-core shell model with continuum

- No-core shell model (NCSM):
 - A-nucleon wave function expansion in the harmonic-oscillator (HO) basis
 - Short- and medium-range correlations
 - Bound states and narrow resonances
- NCSM with Resonating Group Method (NCSM/RGM):
 - Cluster expansion
 - Proper asymptotic behavior
 - Long-range correlations



The most efficient:
**No-Core Shell Model with Continuum
(NCSMC)**

S.Baroni, P. Návratil, S.Quaglioni
 PRL 110, 022505 (2013)

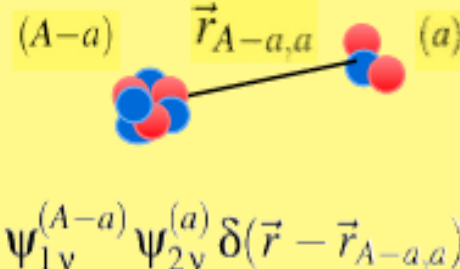
$$\Psi^{(A)} = \sum_{\lambda} c_{\lambda} \underbrace{\left| (A) \text{ (two nucleons), } \lambda \right\rangle}_{\text{NCSM eigenstates}} + \sum_{\nu} \int d\vec{r} \gamma_{\nu}(\vec{r}) \hat{A}_{\nu} \underbrace{\left| (A-a) \text{ (one nucleon), } \nu \right\rangle}_{\text{NCSM/RGM channel states}}$$

Unknowns

The *ab initio* NCSM-RGM equation

- Ansatz:

$$\Psi^{(A)} = \sum_v \int d\vec{r} \varphi_v(\vec{r}) \hat{\mathcal{A}} \Phi_{v\vec{r}}^{(A-a,a)}$$



eigenstates of
 $H_{(A-a)}$ and $H_{(a)}$
in the *ab initio*
NCSM basis

- Many-body Schrödinger equation:

$$H\Psi^{(A)} = E\Psi^{(A)}$$

$$T_{\text{rel}}(r) + \mathcal{V}_{\text{rel}} + \bar{V}_{\text{Coul}}(r) + H_{(A-a)} + H_{(a)}$$

$$\sum_v \int d\vec{r} \left[\mathcal{H}_{\mu\nu}^{(A-a,a)}(\vec{r}', \vec{r}) - E \mathcal{N}_{\mu\nu}^{(A-a,a)}(\vec{r}', \vec{r}) \right] \varphi_v(\vec{r}) = 0$$

realistic nuclear Hamiltonian

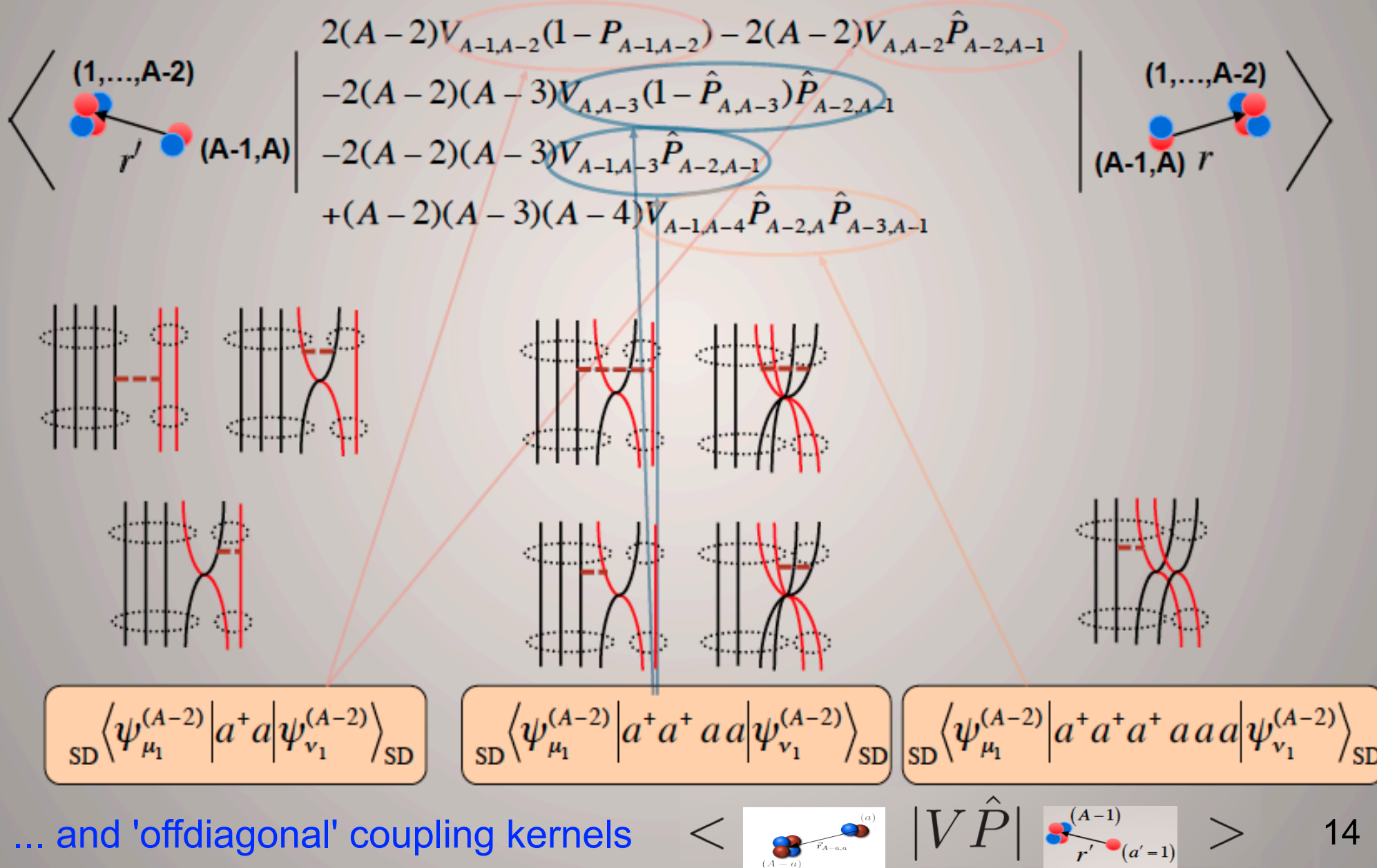
$$\langle \Phi_{\mu\vec{r}'}^{(A-a,a)} | \hat{\mathcal{A}} H \hat{\mathcal{A}} | \Phi_{v\vec{r}}^{(A-a,a)} \rangle$$

Hamiltonian kernel

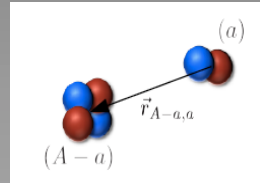
$$\langle \Phi_{\mu\vec{r}'}^{(A-a,a)} | \hat{\mathcal{A}}^2 | \Phi_{v\vec{r}}^{(A-a,a)} \rangle$$

Norm kernel

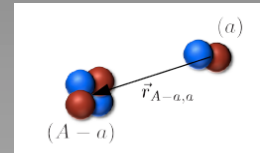
The deuteron projectile: Hamiltonian kernel



Three-body density Hamiltonian kernel



$$\left\langle \Phi_{k'_{ab}}^{J^\pi T} \right| \left(V_{A,A-4} \hat{P}_{A-2,A-1} \hat{P}_{A-3,A} \right) \left| \Phi_{k_{ab}}^{J^\pi T} \right\rangle$$



$$\underbrace{\text{SD} \langle A-2\alpha' | \hat{a}_{\beta_{A-4}}^\dagger \hat{a}_a^\dagger \hat{a}_b^\dagger \hat{a}_{b'}^\dagger \hat{a}_{\beta'_{A-3}} \hat{a}_{\beta'_{A-4}} | A-2\alpha \rangle}_{\text{Three-body density matrix}} \underbrace{\text{SD} a \langle \beta_{A-4}, a' | V_{A,A-4} | \beta'_{A-4} \beta'_{A-3} \rangle_a}_{\text{Two-body potential}}$$

- Number of three-body matrix elements increases fast with basis size
- Optimized numerical algorithm: On-the-fly calculation of the needed three-body matrix elements for a given target nucleus in the m-scheme

Memory size issue in kernels computation

Dimension of the RGM kernels affects the calculation:

- › Memory of a node could be insufficient to handle kernels files
- › R-matrix solver is slowed down by the reading-in of huge kernel files

Three different 'representations' of the three-body kernels:

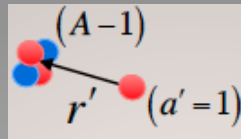
$$1) \langle A-2\alpha'_1 I'_1 M'_1 T'_1 M'_{T_1} | \hat{a}_{\beta_{A-4}}^\dagger \hat{a}_{n_a \ell_a j_a m_{j_a}}^\dagger \frac{1}{2} m_{t_a} | \hat{a}_{n_b \ell_b j_b m_{j_b}}^\dagger \frac{1}{2} m_{t_b} | \hat{a}_{n'_b \ell'_b j'_b m'_{j'_b}}^\dagger \frac{1}{2} m'_{t'_b} | \hat{a}_{\beta'_{A-3}}^\dagger \hat{a}_{\beta'_{A-4}} | A-2\alpha_1 I_1 M_1 T_1 M_{T_1} a \rangle_{SD}$$

$$2) \left\langle \Phi_{k'_{ab}}^{J^\pi T} \right| \left(V_{A,A-4} \hat{P}_{A-2,A-1} \hat{P}_{A-3,A} \right) \left| \Phi_{k_{ab}}^{J^\pi T} \right\rangle$$

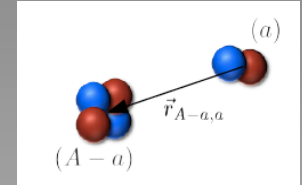
$$3) \left\langle \Phi_{\nu' r'}^{J^\pi T} \right| \left(V_{A,A-4} \hat{P}_{A-2,A-1} \hat{P}_{A-3,A} \right) \left| \Phi_{\nu r}^{J^\pi T} \right\rangle$$

Nmax (single-channel d - ${}^4\text{He}$)	1) # 3-body density matrix	2) # Kernels in SD-basis	3) # Kernels in physical basis
2	$\sim 10^5$	$\sim 10^2$	20
4	$\sim 10^7$	$\sim 10^3$	70
6	$\sim 10^9$	$\sim 10^4$	167
8	$\sim 10^{10}$	$\sim 10^5$	325

Coupling Hamiltonian kernel



$$\left\langle \Phi_{k'_a}^{J^\pi T} \right| \left(V_{A-3,A-2} \hat{P}_{A-2,A} \right) \left| \Phi_{k_{ab}}^{J^\pi T} \right\rangle$$



$${}_{SD}\langle A-1\alpha' | \hat{a}_{\beta_{A-3}}^\dagger \hat{a}_b^\dagger \hat{a}_a^\dagger \hat{a}_{\beta'_{A-2}} \hat{a}_{\beta'_{A-3}} | A-2\alpha \rangle_{SD} {}_a\langle \beta_{A-3}, a' | V_{A-3,A-2} | \beta'_{A-3} \beta'_{A-2} \rangle_a$$

“Not-diagonal” density matrix Two-body potential

(A-2,2) mass partition in the entrance channel
 (A-1,1) mass partition in the exit channel

- Inclusion of coupling kernel describing the dominant channel in a (*d,p/n*) transfer reaction

$\langle d, {}^7\text{Li} | {}^9\text{Be} \rangle$ & $\langle p, {}^8\text{Li} | {}^9\text{Be} \rangle$ cluster overlaps

N_{max} = 6

- Understand cluster structure of ${}^9\text{Be}$

Cluster overlaps from NCSM eigenstates

$$g(r) = \langle \Psi^{(A)} | \mathcal{A} \Psi^{(A-a)} \Psi^{(a)} \delta_{r,r_{A,A-a}} \rangle$$

$\langle {}^9\text{Be} | p + {}^8\text{Li} \rangle$ E_{thr} = -37.60 MeV

J ^π T	E (${}^9\text{Be}$) [MeV]	(2s,l)	S
$(3/2^+1/2)_5$	4.49	$(3,0)^*$	0.356
$(5/2^-1/2)_6$	3.87	$(5,1)^*$	0.052
$(5/2^+1/2)_4$	3.46	$(5,0)$	0.593

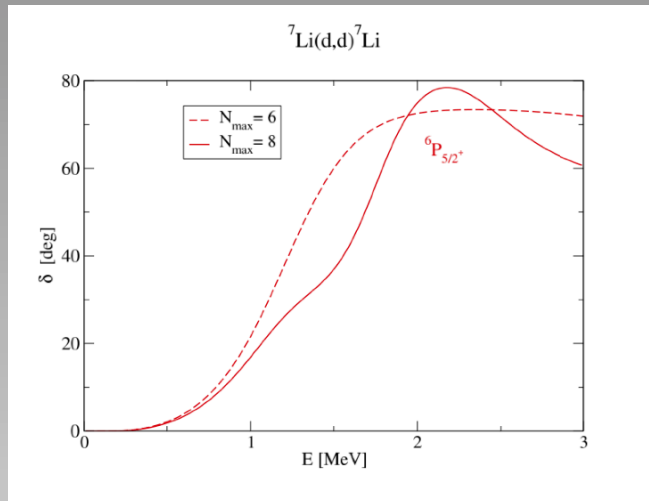
Large overlap of mass partitions considered with compound nucleus in the $5/2^+$ partial wave

$\langle {}^9\text{Be} | d + {}^7\text{Li} \rangle$ E_{thr} = -38.16 MeV

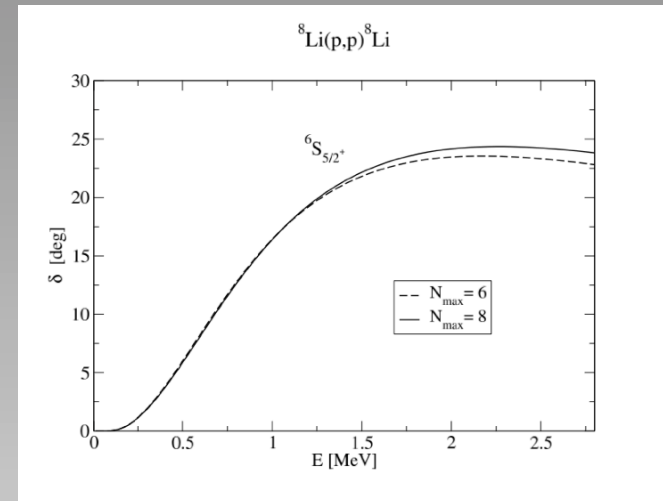
J ^π T	E (${}^9\text{Be}$) [MeV]	(2s,l)	S
$(1/2^-1/2)_4$	2.98	$(1,0)^*$	0.140
$(5/2^-1/2)_6$	4.43	$(5,0)^*$	0.153
$(5/2^+1/2)_4$	3.46	$(5,1)$	0.371

Phase shifts analysis (NCSM-RGM)

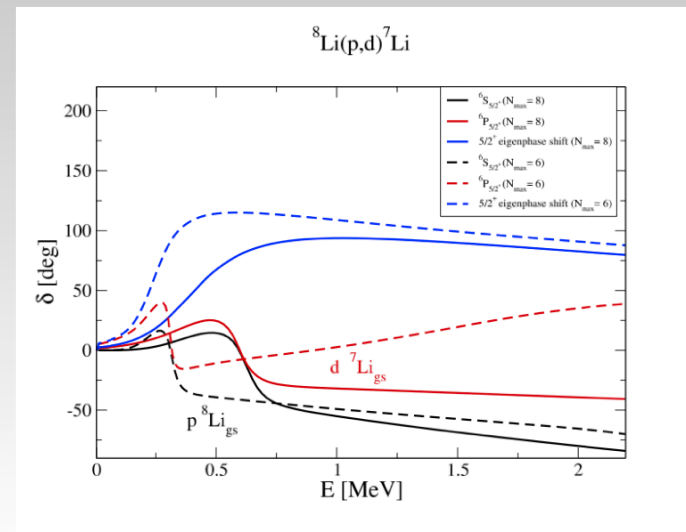
Analysis of the partial wave phase shifts: spin and parity (J^π) of the resonance



$J^\pi = 5/2^+$
dominant
resonance
at low energy

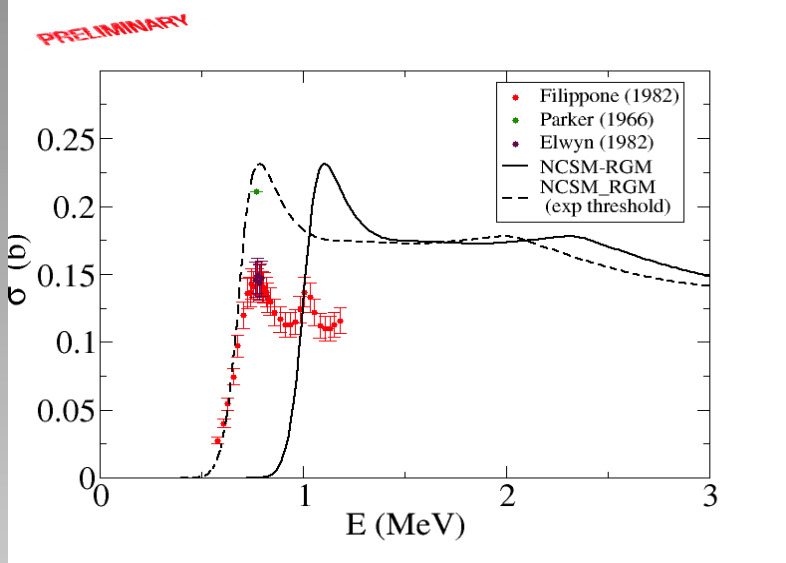


Effect of the coupling:
contribution from
'offdiagonal' elements of
the collision matrix



Eigenphase shifts convey informations on all the matrix elements of the collision matrix

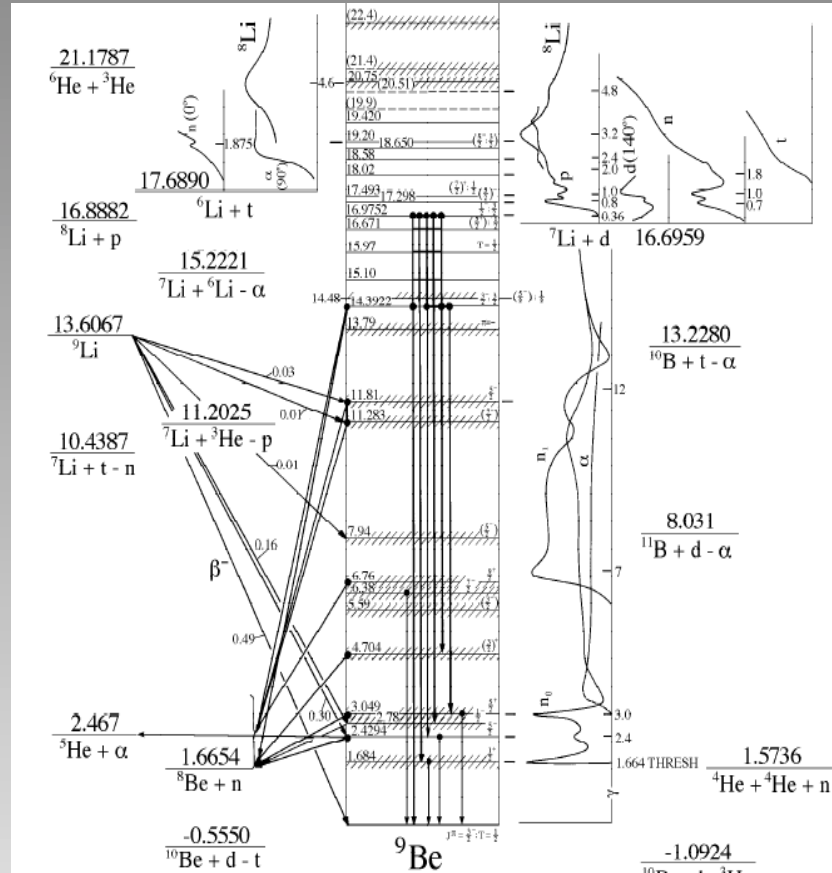
$^7\text{Li}(d,p)^8\text{Li}$ scattering results (NCSM-RGM)



Included channels:

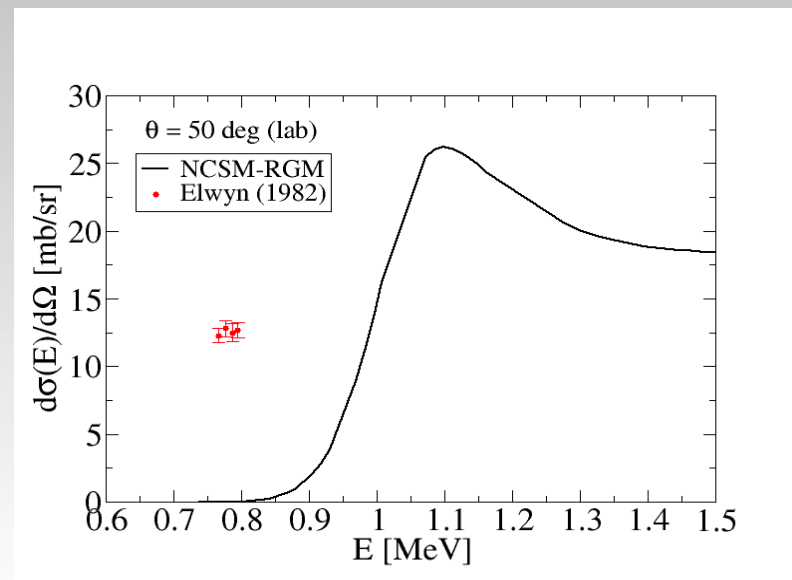
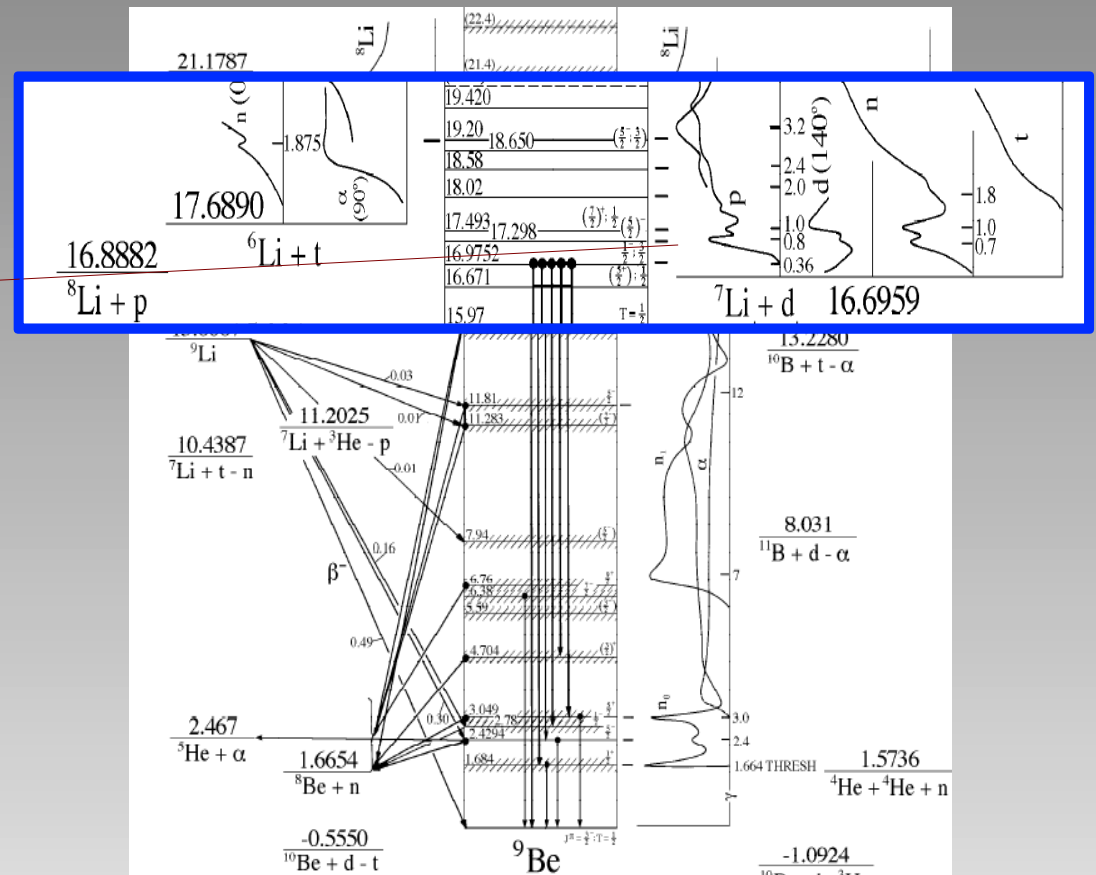
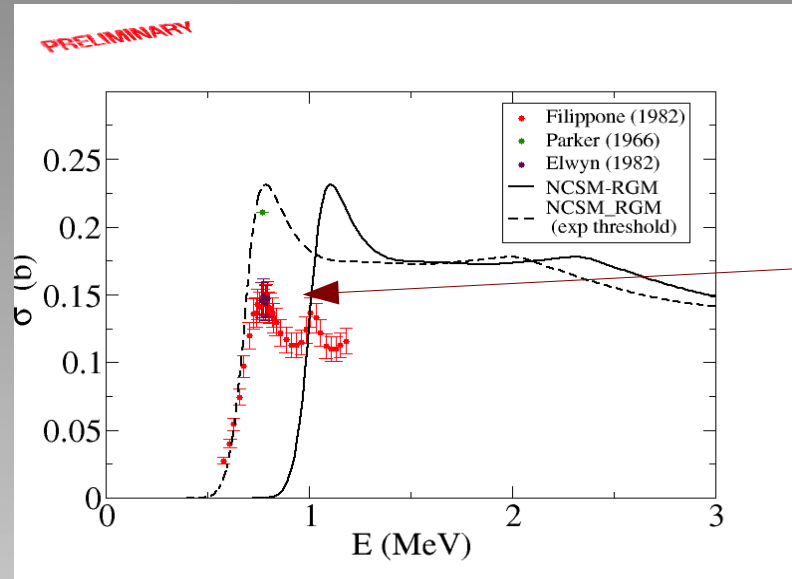
- (1) $p, ^8\text{Li}$
- (2) $d, ^7\text{Li}$
- (3) coupling (d,p)
- (4) virtual breakup of d

Not-included channels: (1) $^8\text{Be}, n$ (2) $^6\text{Li}, t$



NCSM-RGM calculations with chiral N³LO NN potentials (SRG $\lambda=2.02 \text{ fm}^{-1}$)
 4 eigenstates of ^8Li , 2 eigenstates of ^7Li and 5 pseudostates of deuteron
 Preliminary: Nmax=6, $\hbar\Omega=20 \text{ MeV}$

$^7\text{Li}(d,p)^8\text{Li}$ scattering results (NCSM-RGM)

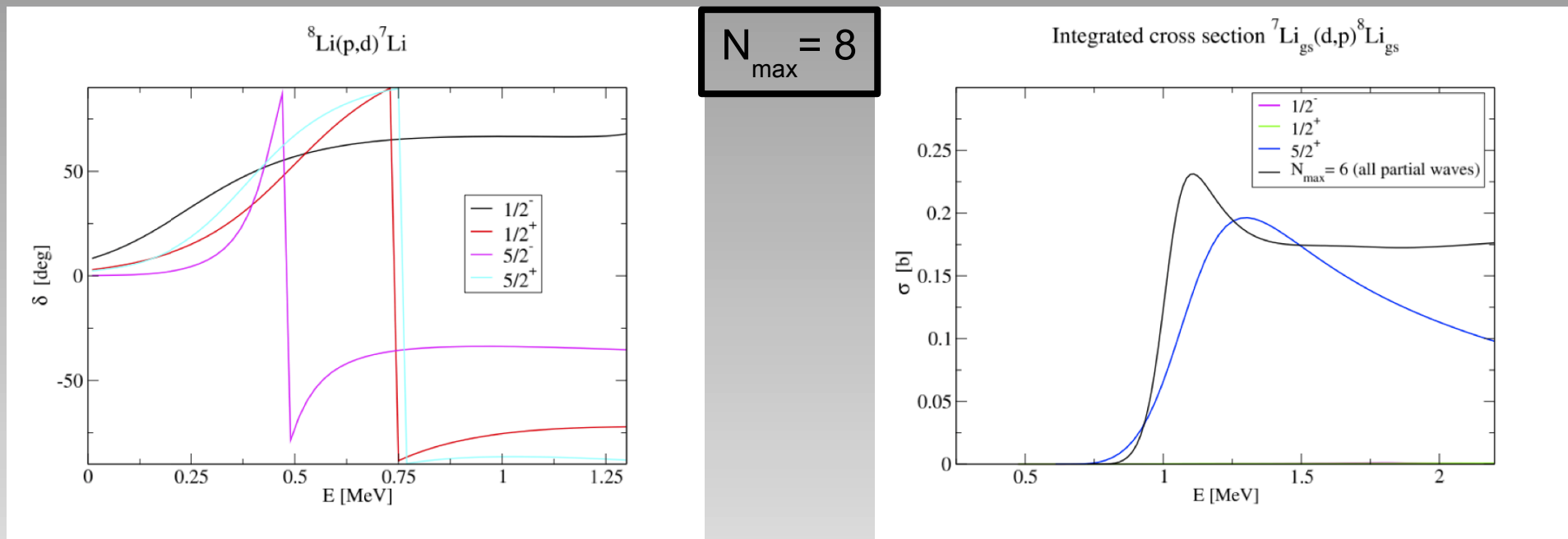


Lowest peak in the experimental total cross section:
 $(E(5/2^-) \sim 0.8 \text{ MeV above the threshold})$

(Uncertain spin-parity assignment)

Impact of $5/2^+$ resonance on cross section

Cross section calculated from selected partial waves:

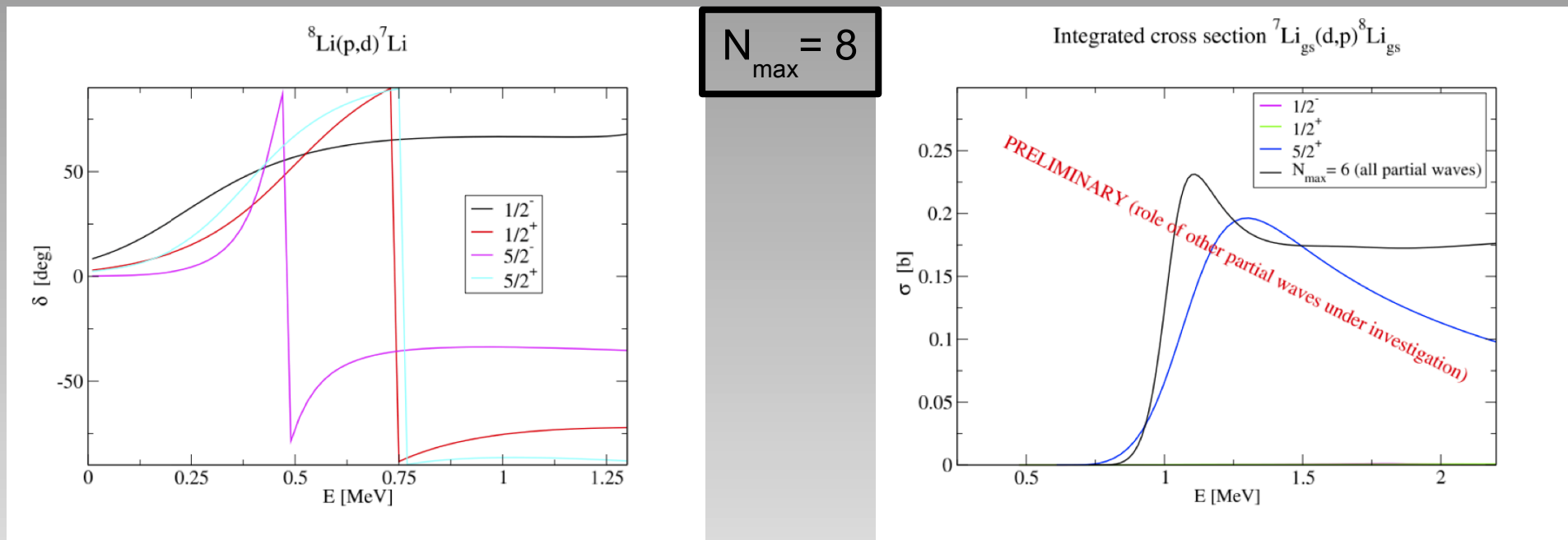


Main eigenphase shifts at low energy of deuteron: $5/2^+$ stable when increasing the model space dimension

$5/2^+$ partial wave accounts for most of the strength of the first resonance above the d - ${}^7\text{Li}$ thresholds.

Impact of $5/2^+$ resonance on cross section

Cross section calculated from selected partial waves:

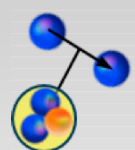
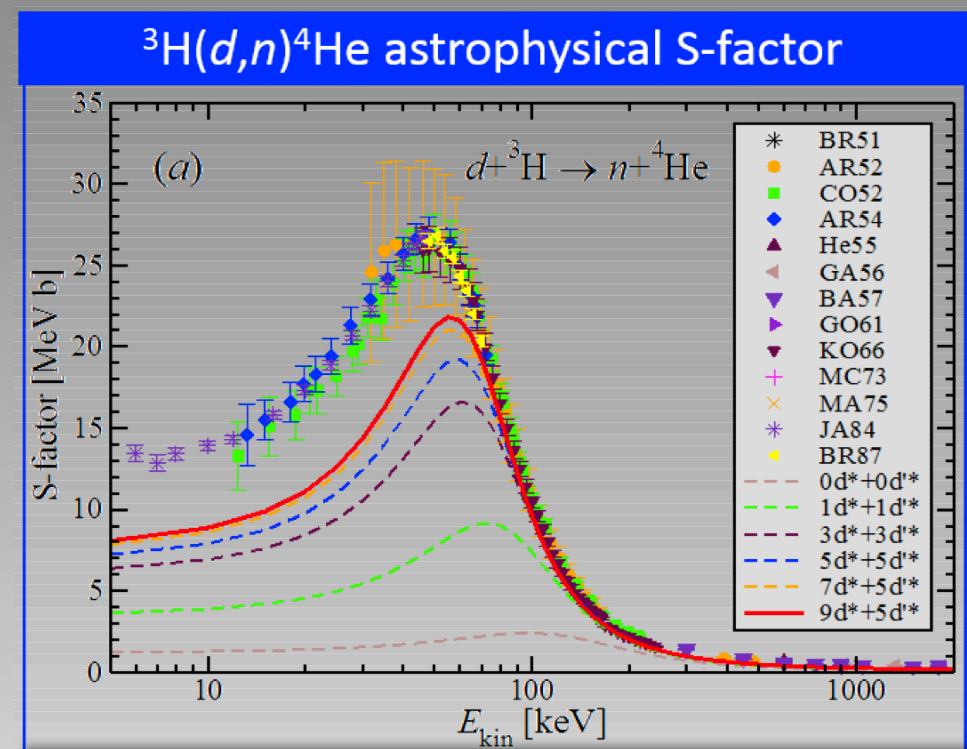
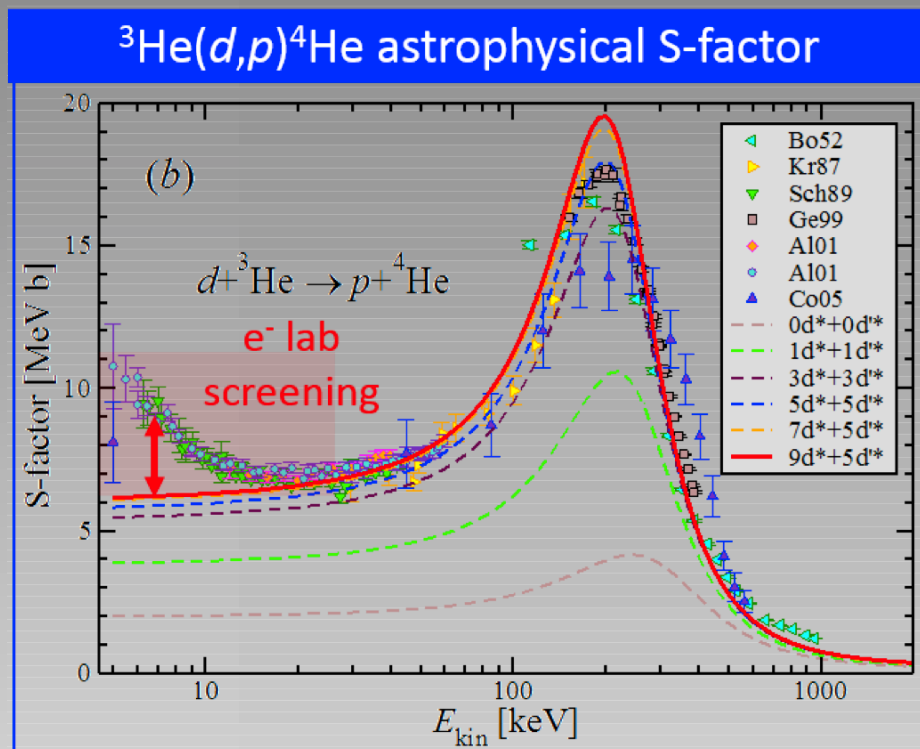


Main eigenphase shifts at low energy of deuteron: $5/2^+$ stable when increasing the model space dimension

$5/2^+$ partial wave accounts for most of the strength of the first resonance above the d - ${}^7\text{Li}$ thresholds.



TRIUMF First step towards *ab initio* calculation transfer reactions (Navrátil, Quaglioni PRL108, 2012)



Deuterium breakup:

Calculated S-factors converge with the inclusion of virtual breakup of the Deuterium, obtained by means of excited ${}^3\text{S}_1$ - ${}^3\text{D}_1(d^*)$ and ${}^3\text{D}_2(d^*)$ pseudostates

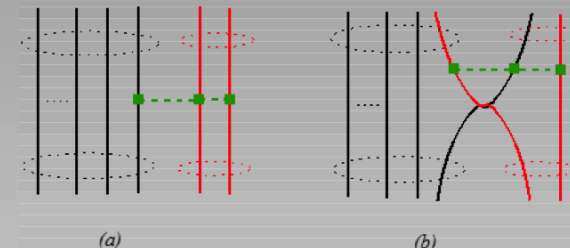
NCSM/RGM results for the ${}^3\text{He}(d,n){}^4\text{He}$ astrophysical S-factor compared to beam-target measurements.

Incomplete nuclear interaction:
Requires 3N forces (SRG-induced
+ “real”)

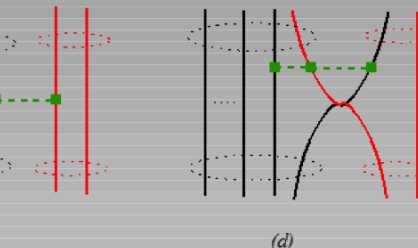
Including 3N force into the description of deuteron-nucleus scattering

$$\left\langle \Phi_{v' r'}^{J^{\pi_T}} \left| \hat{A}_{v'} V^{NNN} \hat{A}_v \right| \Phi_{v r}^{J^{\pi_T}} \right\rangle = \left\langle \begin{array}{c} (A-2) \\ \vec{r}' \\ (a'=2) \end{array} \right| V^{NNN} \left(1 - \sum_{i=1}^{A-2} \sum_{k=A-1}^A \hat{P}_{ik} + \sum_{i < j=1}^{A-2} \hat{P}_{iA-1} \hat{P}_{jA} \right) \left| \begin{array}{c} (A-2) \\ \vec{r} \\ (a=2) \end{array} \right\rangle$$

Direct {

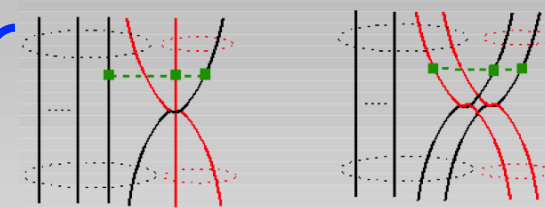


(c)



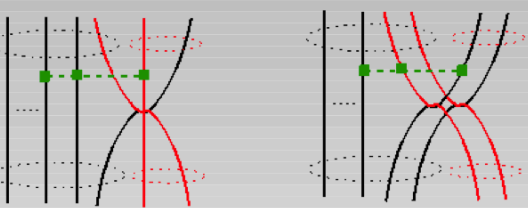
(d)

Exchange {



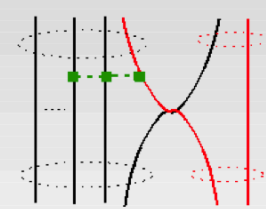
(e)

(f)

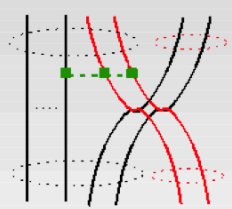


(g)

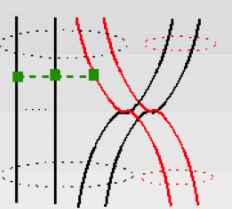
(h)



(i)



(j)



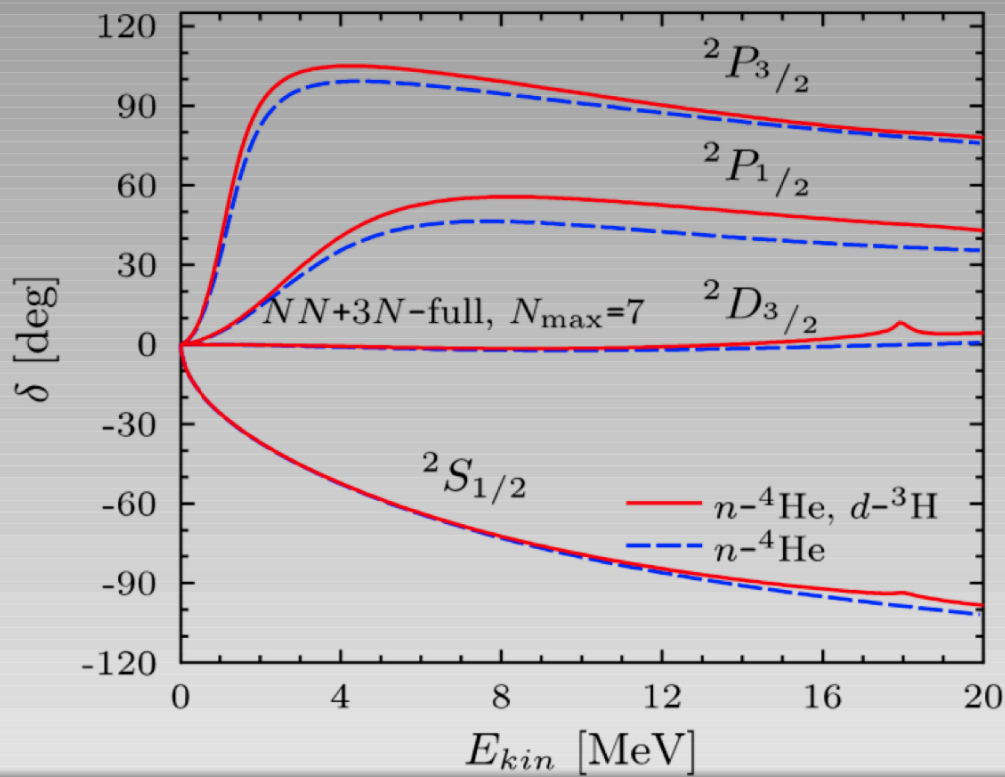
(l)



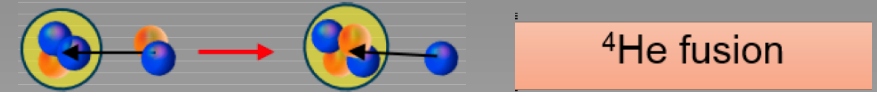
Four body
density

NCSM-RGM calculation of transfer reaction ${}^3\text{H}(d,n){}^4\text{He}$ with 3N forces

$n-{}^4\text{He}$ with the $d-{}^3\text{H}$ channel with the chiral two- and three-nucleon force (preliminary)



$n+{}^4\text{He(g.s.)}$ phase shifts with NN+3N potential, $\lambda=2.0$ fm $^{-1}$, no ${}^5\text{He}$ eigenstates, with/o coupling to d-t.

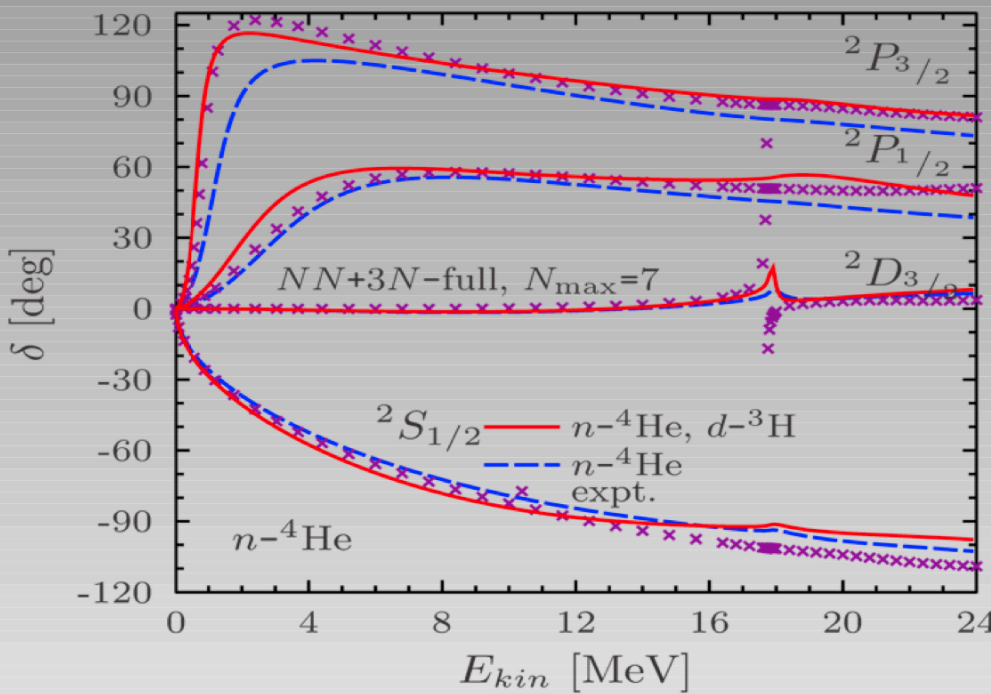


- Perspective to provide accurate $t(d,n){}^4\text{He}$ fusion cross-section for the effort toward earth-based fusion energy generation
- The $d-t$ transfer is known to be very sensitive to the spin-orbit and tensor part of the nuclear interaction

- 7 diagrams (+ exchange) arising from the coupling of $n-\alpha$ with $d-t$ through the three-nucleon force.
- Next step: Coupling to the compound ${}^5\text{He}$ eigenstates

NCSMC calculation of transfer reaction $^3\text{H}(d,n)^4\text{He}$ with 3N forces

^4He fusion with NCSMC and the chiral two- and three-nucleon force (preliminary)



$n+^4\text{He(g.s.)}$ phase shifts with NN+3N potential, $\lambda=2.0$ fm $^{-1}$, with eigenstates of ^5He .



^4He fusion

- Perspective to provide accurate $t(d,n)^4\text{He}$ fusion cross-section for the effort toward earth-based fusion energy generation
- The d - t transfer is known to be very sensitive to the spin-orbit and tensor part of the nuclear interaction

- Preliminary, small $N_{MAX} = 7$

Conclusions & Perspectives

First application of the NCSM-RGM for deuteron-projectile and p-shell nucleus as target:

- Inclusion of the “elastic” and coupling channel in the description of transfer reactions

Analysis of the ${}^9\text{Be}$ resonances above $d\text{-}{}^7\text{Li}$ threshold:

- Discussion of the spin-parity assignment of 0.78 MeV resonance

RGM and NCSMC results on $d\text{-t}$ and $d\text{-}{}^3\text{He}$ transfer reaction with 3N force

To be done:

- Complete the calculation ($N_{\text{max}}=8$) of the ${}^7\text{Li}(d,p){}^8\text{Li}$ transfer reaction in NCSM-RGM and NCSMC
- Include 3N force also for p-shell nuclei